

Diffraction characteristics analysis of multi-depth phase modulation grating in terahertz band

YANG Qiu-jie, HE Zhi-ping, MI Zhong-liang

Citation:

YANG Qiu-jie, HE Zhi-ping, MI Zhong-liang. Diffraction characteristics analysis of multi-depth phase modulation grating in terahertz band[J]. *Chinese Optics*, 2020, 13(3): 605–615. doi: 10.3788/CO.2019-0147

杨秋杰, 何志平, 糜忠良. 太赫兹立体相位光栅衍射特性分析[J]. *中国光学*, 2020, 13(3): 605–615. doi: 10.3788/CO.2019-0147

View online: <https://doi.org/10.3788/CO.2019-0147>

Articles you may be interested in

[Recent advances in terahertz digital holography](#)

太赫兹数字全息术的研究进展

Chinese Optics. 2017, 10(1): 131 <https://doi.org/10.3788/CO.20171001.0131>

[Terahertz atmosphere remote sensing](#)

太赫兹大气遥感技术

Chinese Optics. 2017, 10(5): 656 <https://doi.org/10.3788/CO.20171005.0656>

[Terahertz-wave devices based on plasmons in two-dimensional electron gas](#)

二维电子气等离激元太赫兹波器件

Chinese Optics. 2017, 10(1): 51 <https://doi.org/10.3788/CO.20171001.0051>

[Optically controlled narrowband terahertz switcher based on graphene](#)

基于石墨烯的光学控制窄带太赫兹开关

Chinese Optics. 2018, 11(2): 166 <https://doi.org/10.3788/CO.20181102.0166>

[Development of ultra high sensitivity superconducting THz detectors](#)

超高灵敏度太赫兹超导探测技术发展

Chinese Optics. 2017, 10(1): 122 <https://doi.org/10.3788/CO.20171001.0122>

[Advances in organic nonlinear crystals and ultra-wideband terahertz radiation sources](#)

新型有机晶体及超宽带太赫兹辐射源研究进展

Chinese Optics. 2019, 12(3): 535 <https://doi.org/10.3788/CO.20191203.0535>

Diffraction characteristics analysis of multi-depth phase modulation grating in terahertz band

YANG Qiu-jie¹, HE Zhi-ping^{1,2*}, MI Zhong-liang³

(1. Key Laboratory of Space Active Opto-Electronics Technology, Shanghai Institute of Technical Physics, Chinese Academy of Sciences, Shanghai 200083, China;

2. University of Chinese Academy of Sciences, Beijing 100049, China;

3. Shanghai Key Laboratory of Crime Scene Evidence, Shanghai 200000, China)

* Corresponding author, E-mail: hzping@mail.sitp.ac.cn

Abstract: To meet the requirements of terahertz spectral imaging for wide spectral range, high efficiency and real-time detection of spectrometers, a Multi-depth Phase Modulation Grating (MPMG) in terahertz band is proposed. The phase modulation of incident light is realized by introducing optical path difference resulted from the change of groove depth, so that different regions of reflecting terahertz wave front have different phase information. Based on the analysis of the intensity distribution of the diffraction field of the MPMG, the influence of grating parameters on the distribution of the diffraction field is discussed. The diffraction characteristics of the MPMG are verified by experiments. The experiment results indicate that the measurements of the 0th- and ± 1 st-order diffraction efficiency at 0.5 and 0.34 THz obtained by experiment and simulation are in good agreement. It suggests that 0th order diffraction of the MPMG has the ability of splitting light.

Key words: THz; multi-depth phase modulation grating; fraunhofer diffraction; field distribution

太赫兹立体相位光栅衍射特性分析

杨秋杰¹, 何志平^{1,2*}, 糜忠良³

(1. 中国科学院上海技术物理研究所, 中国科学院空间主动光电重点实验室, 上海 200083;

2. 中国科学院大学, 北京 100049;

3. 上海市现场物证重点实验室, 上海 200000)

摘要: 针对太赫兹谱成像对宽光谱、高光能利用率、实时探测分光器件的需求, 提出了一种太赫兹立体相位光栅(MP-

收稿日期: 2019-07-10; 修订日期: 2019-08-10

基金项目: 国家自然科学基金(No. 61905268); 上海市自然科学基金(No. 18ZR1445500); 上海技术物理研究所创新专项基金(No. CX-158); 上海市现场物证重点实验室开放课题基金(No. 2018XCWZK14)

Supported by the National Natural Science Foundation of China (No. 61905268); Natural Science Foundation of Shanghai Province (No. 18ZR1445500); the Innovation Project Fund of Shanghai Institute of Technical Physics (IPFSITP) (No. CX-158); the Opening Project of Shanghai Key Laboratory of Crime Scene Evidence (No. 2018XCWZK14)

MG)分光器件。MPMG 通过刻槽深度的变化引入光程差,实现对入射光的相位调制,从而使反射太赫兹波前的不同区域具有不同的相位信息,其零级衍射光具备分光能力。在分析 MPMG 衍射场光强分布的基础上,讨论了光栅参数对衍射场分布的影响,并通过实验验证了 MPMG 的衍射特性。结果表明,MPMG 各光栅单元在 0.5 THz、0.34 THz 的衍射效率理论值与实测值相吻合,证明了 MPMG 的零级衍射光具备分光能力。

关键词: 太赫兹; 立体相位光栅; 夫琅禾费衍射; 场分布

中图分类号: TP394.1; TH691.9 **文献标志码:** A **doi:** 10.3788/CO.2019-0147

1 Introduction

Due to the lack of active radiation sources and beam-splitting devices with wide spectrum in terahertz band, there are few kinds of spectral imaging instruments in terahertz band. In particular, as the key component of spectral imaging instrument, the optical splitter directly affects the performance, structural complexity, weight and volume of the instrument^[1-3]. The existing optical splitters of visible and infrared spectroscopic instruments include prism, amplitude grating, acousto-optic tuned filter, etc. However, these beam-splitting devices, which are suitable for visible and infrared bands, cannot meet the requirements of spectral detection and imaging in terahertz band. Firstly, as a classical optical splitter, the prism has the advantages of wide free spectrum, simple structure, large amount of light, high energy utilization and easy stray-light suppression. However, with the increase of the wavelength in terahertz band, the penetration of electromagnetic waves will increase and the dispersion of materials will become extremely weak. This means that it is no longer feasible to obtain fine spectra by material dispersion in terahertz spectrum detection^[4-5]. Secondly, the beam splitting of amplitude grating depends on the diffraction effect. However, the spectral range of a single grating is limited by the overlap of adjacent secondary diffraction spectra. In order to improve the utilization of light energy, the flare grating is adopted and the limited bandwidth of its wavelength further reduces its free spectral range. The terahertz bandwidth (30 μm ~3 mm) is nearly 6 000 times the visible bandwidth (0.38 μm ~

0.75 μm) and 100 times the infrared bandwidth (0.75 μm ~30 μm)^[6-8]. This determines that the beam-splitting devices in terahertz band must have a wide free spectral range, so the flared grating and amplitude modulated grating are not applicable to terahertz band. Finally, the acousto-optic tuned filter relies on acousto-optic effect to realize diffraction, and has the advantages of small volume, high crystal diffraction rate and large field of view. However, no acousto-optic crystal suitable for terahertz band has been found in the published literature^[9-11].

The weak-signal feature of terahertz detection requires terahertz beam splitter with high energy efficiency. To meet the requirements of terahertz spectral imaging for wide spectral range, high efficiency and real-time detection of spectrometers, a Multi-depth Phase Modulation Grating (MPMG) in terahertz band is proposed in this paper^[12]. The phase modulation of incident light is realized by introducing optical path difference resulted from the change of groove depth, so that different regions of reflecting terahertz wave front have different phase information. The typical characteristic of MPMG is that its 0th-order diffraction light carries the phase information due to groove depth modulation and therefore has the ability of splitting light.

2 Diffraction field distribution of MPMG

The MPMG is composed of a series of grating cells whose groove depths vary in an equal gradient. The one-dimensional MPMG and two-dimensional MPMG, whose structures are shown in Fig. 1(a) and

Fig. 1(b) respectively, are both composed of four grating cells. The groove depths of grating cells, namely h_1, h_2, h_3 and h_4 , vary in an equal gradient. Each grating cell is composed of two pairs of crest reflection planes and groove reflection planes parallel to each other, as shown in Fig. 1(c). There is no difference in performance between one-dimensional MPMG and two-dimensional MPMG, but the latter's structure is compact and conducive to the miniaturization of spectral instruments.

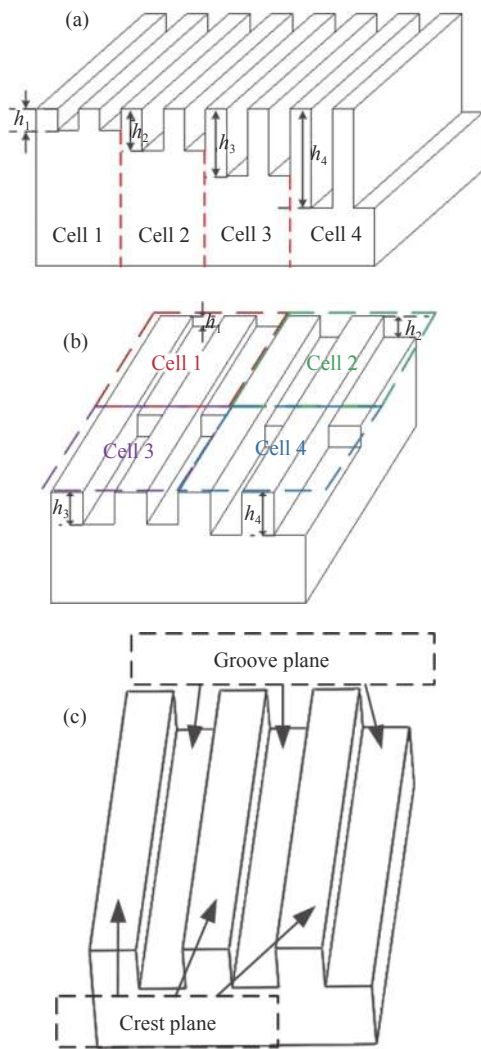


Fig. 1 Schematic diagram of MPMG. (a) 1D MPMG, (b) 2D MPMG, (c) grating cell

图 1 MPMG 示意图 (a) 一维 MPMG, (b) 二维 MPMG (c) 光栅单元

The grating cells are equivalent to a series of planes staggered by different phase differences, as

shown in Fig. 2. When the beam is obliquely incident to the MPMG, the angle between the projection of the wave vector \vec{k} on the plane (x, z) and the vector \vec{k} is ψ , and the angle between this projection and the axis x is θ . The phase difference thereby introduced to the crest reflection planes and groove reflection planes is:

$$\varphi = \frac{4\pi h}{\lambda \cos \psi \sin \theta}. \quad (1)$$

When the terahertz wave is incident in the direction parallel to the paper, that is $\psi=0$, the normalized light intensity distribution after the MPMG diffraction is shown in Eq. (2). The crest reflection planes and groove reflection planes are considered to be with the same width during calculation.

$$I(P_i) = \text{sinc}^2\left(\frac{kl \sin \beta}{2}\right) \text{sinc}^2\left(\frac{kw \sin \alpha}{2}\right) \frac{\sin^2\left[\frac{nk d \sin \alpha}{2}\right]}{\sin^2\left(\frac{kd \sin \alpha}{2}\right)} \cos^2\left(\frac{kw \sin \alpha + \varphi}{2}\right). \quad (2)$$

α and β represent the diffraction angle in the x direction and the diffraction angle in the y direction respectively; \vec{k} is the wave vector; w is the width of crest reflection planes and groove reflection planes; l is the grating length; and n is the number of crest reflection plane and groove reflection plane pairs.

$\text{sinc}^2\left(\frac{kl \sin \beta}{2}\right)$ and $\text{sinc}^2\left(\frac{kw \sin \alpha}{2}\right)$ are used to describe the rectangular aperture diffraction factor, which has a maximum value in 0th-order diffraction;

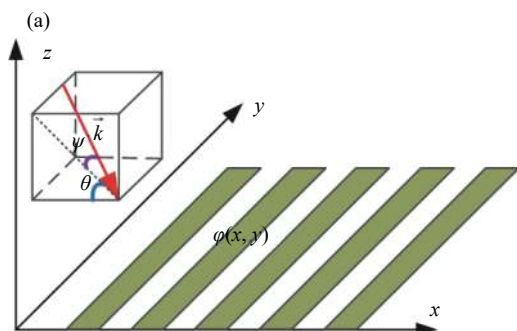
$\frac{\sin^2\left[\frac{nk d \sin \alpha}{2}\right]}{\sin^2\left(\frac{kd \sin \alpha}{2}\right)}$ is used to describe the multiple-beam interference factor. So the grating equation of MPMG is

$$d \sin \alpha = m \lambda, \quad d = w + c, \quad m = 0, \pm 1, \pm 2, \dots \quad (3)$$

That is, the diffraction order distribution of the grating only depends on the grating constant d . When the diffraction light with the same order, the

higher d corresponds to a larger diffraction angle.

$\cos^2\left(\frac{kw \sin \alpha + \varphi}{2}\right)$ represents the modulation of



the additional phase introduced by groove depth on diffraction field intensity.

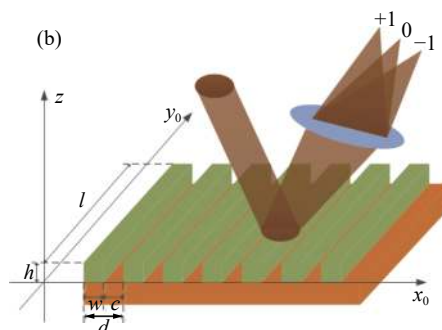


Fig. 2 (a) Reflection grating simulated as a plane transmission grating; (b) MPMG diffraction diagram

图 2 (a) MPMG 等效为平面透射光栅示意图 (b) MPMG 衍射示意图

3 Analysis of MPMG diffraction characteristics

As known from Eq. (3), the intensity distribution of diffraction field along the X -axis is related to

the grating constant d ($d=2w$), the number of crest reflection plane and trough reflection plane pairs (n), and the groove depth (h). The Fig. 3 (color on-line) depicts the distribution of Fraunhofer diffraction field along the X -axis under different design parameter conditions. As can be seen from Figs. 3(a),

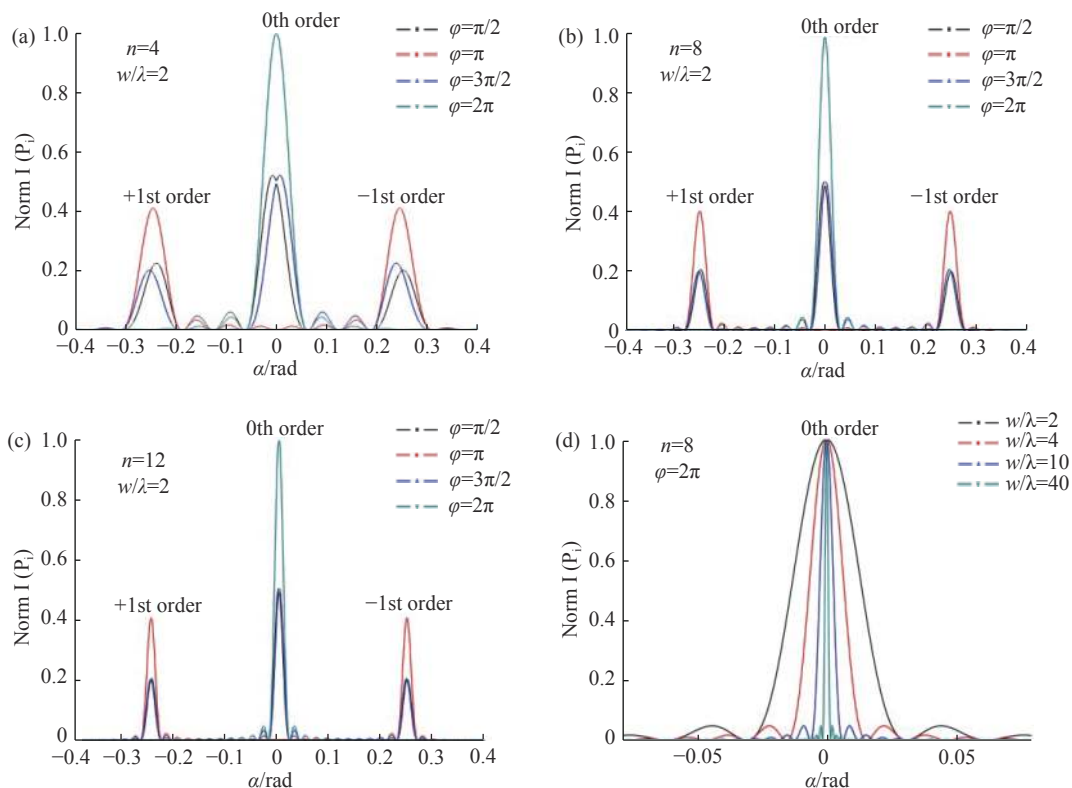


Fig. 3 Light intensity distributions along the x axis under different phase modulation conditions

图 3 不同相位调制下沿 x 轴方向的光强分布

3(b) and 3(c), when only groove depth is variable, the phase modulation introduced by groove depth will enable the energy of diffraction field to shift between level 0th- and ± 1 st-order. When the phase difference φ is 2π , the energy of Fraunhofer diffraction field is all concentrated at the 0th-order; when the phase difference φ is π , the energy of Fraunhofer diffraction field is all concentrated at the ± 1 st-order; when the phase difference φ is $\pi/2$ or $3\pi/2$, the energy of Fraunhofer diffraction field is evenly distributed at the 0th- and ± 1 st-order. The comparison of Figs. 3(a), 3(b) and 3(c) show that, with the increase of crest reflection plane and groove reflection plane pairs, the flare angle of each diffraction order will decrease. The number of crest reflection plane and trough reflection plane pairs is independent of the diffraction angle of each diffraction order. When discussing the effect of the grating constant d ($d=2w$) on diffraction field distribution, w/λ is chosen to avoid the influence of the introduced wavelength. As can be seen from Fig. 3(d), with the increase of w/λ , the primary maximum angular width and diffraction angle of each diffraction order will decrease and the diffraction phenomenon will become less obvious.

4 Testing of MPMG diffraction characteristics

We established a set of experimental facilities for evaluating the diffraction characteristics of MPMG in the laboratory, including a high-power THz radiation source system, Fig. 4(a), a THz laser collimation and transmission system Fig. 4(b) and a grating testing system, as shown in Fig. 4(c). In the Fig. 4, the Lens 1 and Lens 2 constitute a set of beam expanders that represent the collimation and transmission path of the system; and the Lens 3, Lens 4, MPMG and Lens 5 constitute the testing light path of MPMG diffraction characteristics. In the experiment, a tunable Optical Parametric Oscillator (OPO) with the wavelength of 1 066-1 078 nm

and a 1 064 nm Nd:YAG laser were used to produce high-power THz radiation under difference frequency effect^[13], as shown in Fig. 4(a). The spot size of the pumped laser beam is about 4 mm. This THz laser beam produced by nonlinear difference frequency effect is different from a visible or infrared laser beam. Laser Gaussian beam can be treated as parallel light under the following two conditions: first, the radius of beam waist is much larger than the laser wavelength; second, the wavefront radius is much larger than the laser wavelength. Under the former condition, the spot size will remain approximately unchanged during the laser transmission; under the latter condition, the laser wavefront can be approximated to a plane. The wavelength of THz laser is equivalent to the size of beam waist, and the spot size of THz laser is approximately proportional to the transmission distance^[14]. The divergence angle of self-made difference-frequency THz source obtained through experimental measurement is 12° . Therefore, in the experiment, a lens group was used to collimate the THz beams in the optical path shown in Fig. 4(b). The lens group is equivalent to a set of beam expanders in the Fig. 4(c)^[15-16]. After being collimated by the lens group, the divergence angle of THz laser beam is 0.1° . The grating test system consists of three high density polyethylene lenses, a rectangular stop, a MPMG and a THz detector, as shown in Fig. 4(e). The 1D MPMG used in the experiment is composed of 8 grating cells, each of which includes five pairs of crest planes and groove planes. The MPMG parameters are given in Table 1 and the MPMG picture is shown in Fig. 4(d). The THz detector used in the experiment is the second generation of quasi-optical detector (2dl 12c LS 2500 A1) purchased from Advanced Compound Semiconductor Technologies (ACST, Hanau, Germany). The photosensitive surface of the detector is encapsulated with a convergence mirror with a diameter of 2 mm to achieve higher light-energy collection efficiency, as shown in Fig. 4(f).

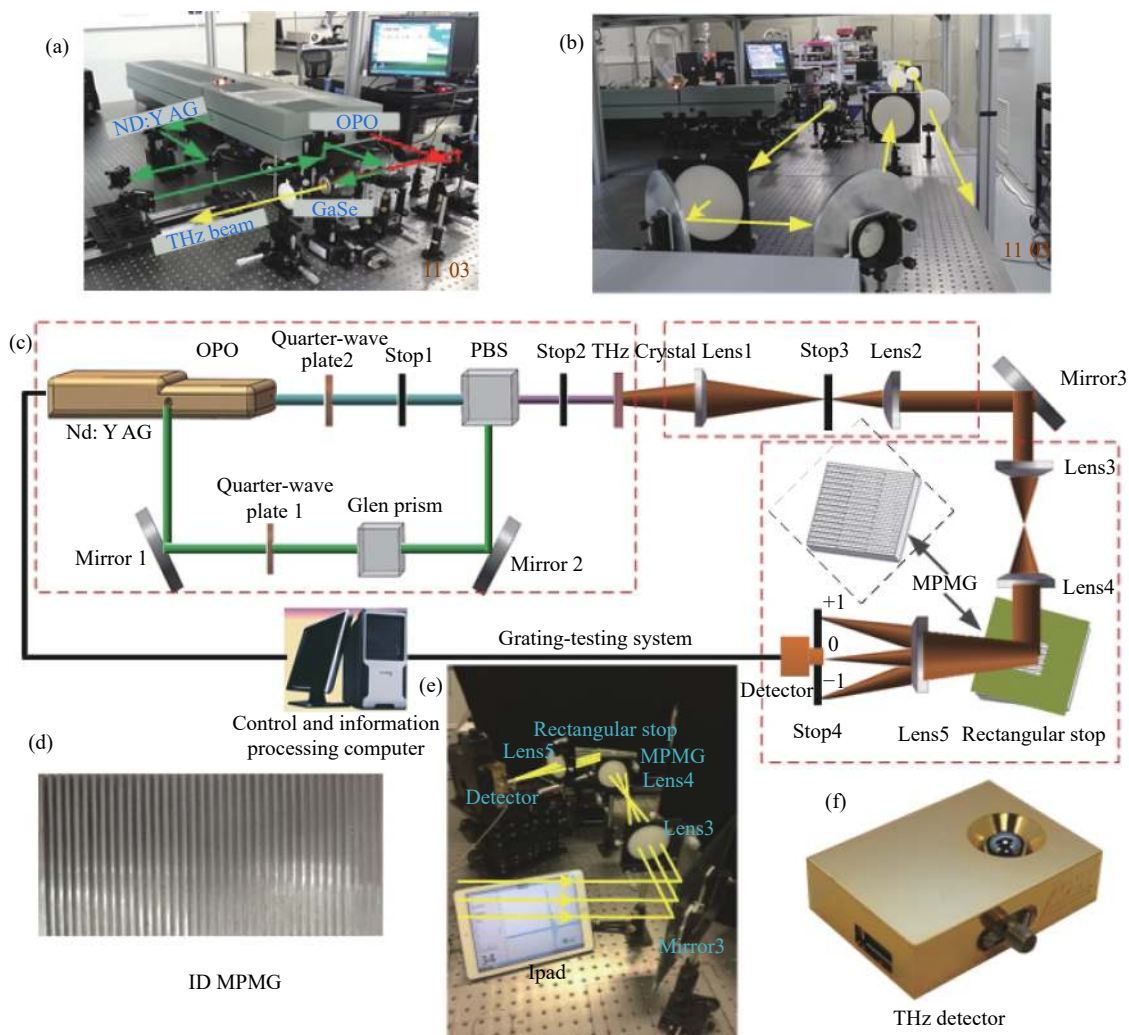


Fig. 4 (a) High-power THz radiation source system. (b) Laser collimation and transmission system. (c) Schematic of experiment. (d) 1D MPMG. (e) Grating-testing system. (f) Photograph of the THz detector.

图 4 (a) 高功率辐射源系统; (b) 激光准直与发射系统; (c) 实验方案; (d) 一维 MPMG; (e) 光栅测试系统; (f) 探测器照片

Tab. 1 Parameters of 1D MPMG

表 1 一维 MPMG 参数

Name of parameter	Value	Name of parameter	Value
N	8	n	5
w/mm	1	l/mm	40
$\psi/(\text{°})$	0	$\theta/(\text{°})$	60
h/cm			
$h\{1\}$	0.163 5	$h\{5\}$	0.817 5
$h\{2\}$	0.327 0	$h\{6\}$	0.981 0
$h\{3\}$	0.490 5	$h\{7\}$	1.144 5
$h\{4\}$	0.654 0	$h\{8\}$	1.308 0

The test method is described below. After being collimated by the lens group, the 0.5 THz radiation is parallelly incident to and diffracted by the MPMG ($\theta = 60^\circ$, $\psi = 0^\circ$). After being converged by the THz lens, the diffracted waves at the 0th- and ± 1 st-order are detected by the THz detector in the focal plane of the lens. A thin rectangular stop is placed on the front surface of the MPMG to ensure that only one cell is effectively illuminated by each incident THz wave. By moving the detector in proper order, the diffraction intensities at the 0th- and ± 1 st-order can be recorded. By repeating this operation for each grating cell, the intensities of all the

grating cell at the 0th- and ± 1 st-order can be obtained. In order to eliminate the influence of laser jitter on the measurement results, the measurement results of multiple tests (20 measurements) are averaged. By normalizing the measured data, the 0th- and ± 1 st-order diffraction efficiencies of 8 grating cells can be obtained.

By changing the OPO wavelength, the diffraction intensity of the 0.34 THz radiation wave in 8 grating cells is measured. The theoretical simula-

tion curves and measurement results of diffraction efficiencies of 0.5 THz and 0.34 THz radiation in the grating cells are shown in Fig. 5. It can be seen that the experimental results are in agreement with the theoretical simulation results, that demonstrates the diffraction characteristics of MPMG, that is, the 0th-order diffracted light of MPMG carries the phase information and its diffraction intensity is modulated by the phase introduced by groove depth.

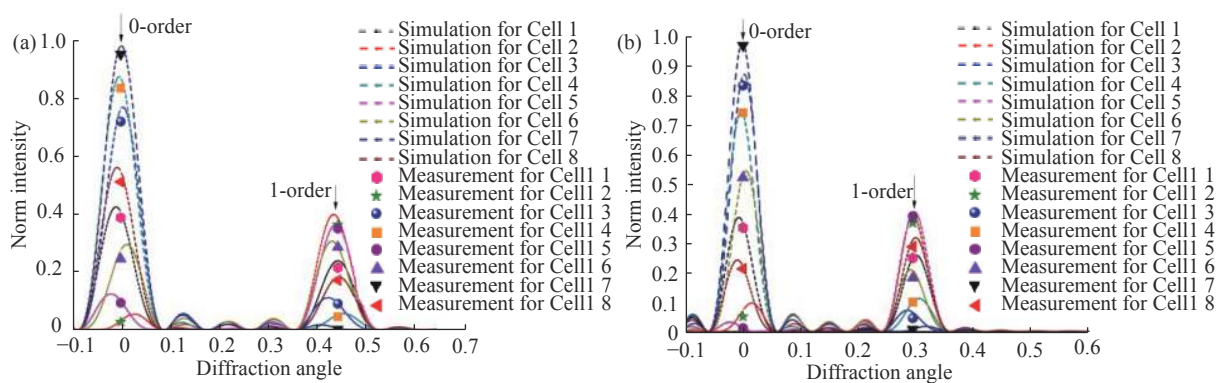


Fig. 5 Simulation and test results of 0th- and 1st-order diffraction efficiency for each grating cell at (a) 0.34 THz and (b) 0.5 THz

图5 光栅单元0级和1级衍射效率的模拟和测试结果 (a) 0.34 THz (b) 0.5 THz

5 Conclusion

In this paper, a new MPMG in THz band, which is composed of a series of grating cells, is presented. The groove-depth gradients of these grating cells correspond to different positions of the moving mirrors in the Fourier transform spectrum system. The calculation results of Fraunhofer diffraction field distribution and diffraction efficiency of MPMG show that, the 0th-order diffracted light

of MPMG carries the phase information and its diffraction intensity is modulated by the phase introduced by groove depth. We develop the MPMG composed of eight grating cells and test its 0th- and 1st-order diffraction efficiencies at 0.5 THz and 0.34 THz. The test results agree well with the simulation results. Therefore, we believe that the 0th-order diffracted light of MPMG carries the phase information and its diffraction intensity is modulated by the phase introduced by groove depth.

——中文对照版——

1 引言

太赫兹波段的光谱成像仪器种类稀少,这是由于太赫兹宽谱主动辐射光源与太赫兹宽谱分光

器件缺乏所共同导致的。其中分光器件作为光谱成像仪器的关键部件,直接影响仪器的性能、结构的复杂程度、重量和体积等^[1-3]。目前,可见、红外光谱仪器的分光器件有:棱镜、振幅光栅、声光调谐滤波器等。然而,这些适用于可见、红外波

段的分光器件并不能满足太赫兹波段物质的谱探测与成像对分光器件的需求。棱镜作为经典的分光器件具有自由光谱范围宽、结构简单、通光量大,能量利用率高,杂散光易于抑制的优点,然而在太赫兹波段,随着波长的增加,电磁波的穿透性能增强,材料的色散现象变的极其微弱,这意味着通过材料色散获取精细光谱的方式在太赫兹谱探测中不在可行^[4-5]。振幅光栅是依靠衍射效应分光的,然而受相邻衍射次级光谱重叠的限制,单块光栅的光谱范围有限,为了提高光能利用率而采用的闪耀光栅,其闪耀波长的带宽有限,进一步缩小了光栅的自由光谱范围。太赫兹(30 μm ~3 mm)的频段带宽是可见(0.38 μm ~0.75 μm)频段带宽的近 6 000 倍,是红外(0.75 μm ~30 μm)频段带宽的 100 倍^[6-8]。这决定了太赫兹波段的分光器件必须具备宽自由光谱范围,因此闪耀光栅、振幅调制光栅不适合用作太赫兹波段的分光器件。声光调谐滤波器依靠声光效应实现衍射分光,其具有体积小,晶体衍射率高、大视场的优点,但目前尚未在公开报道的文献中查阅到适用于太赫兹波段的声光晶体^[9-11]。

若要使太赫兹探测到弱信号,则要求太赫兹分光器件必须具备高能量利用效率。针对太赫兹谱成像对宽光谱、高光能利用率、实时探测分光器件的需求,本文提出一种太赫兹立体相光栅(MPMG)分光器件^[12],通过刻槽深度的变化引入光程差,实现对入射光的相位调制,使反射太赫兹波前的不同区域具有不同的相位信息。该 MPMG 的典型特征在于,槽深调制使 MPMG 的零级衍射光携带相位信息,因此 MPMG 零级衍射光具备分光能力。

2 MPMG 的衍射场分布

MPMG 由槽深呈等梯度变化的一系列光栅单元组成。一维 MPMG、二维 MPMG 的结构示意图分别如图 1(a)、1(b) 所示,二者均由 4 个光栅单元组成,光栅单元的槽深 h_1 、 h_2 、 h_3 、 h_4 呈等梯度变化,光栅单元由两对互相平行的顶、槽反射平面组成,如图 1(c) 所示。一维立体相位光栅和二

维相位光栅在性能上没有差异,但二维相位光栅结构紧凑,利于光谱仪器的小型化。

将光栅单元等效为一系列不同相位差交错排列的平面,如图 2 所示,当光束斜入射 MPMG 时,波矢 \vec{k} 在 (x,z) 平面的投影与 \vec{k} 方向的夹角为 ψ ,波矢 \vec{k} 在 (x,z) 平面的投影与 x 轴的夹角为 θ ,则顶、槽反射面由此引入的相位差为:

$$\varphi = \frac{4\pi h}{\lambda \cos \psi \sin \theta}. \quad (1)$$

当太赫兹波平行于纸面方向入射,即($\psi = 0$)时,经 MPMG 衍射后归一化的光强分布表达式如式 (2) 所示,计算时认为顶反射面和槽反射面的宽度相等。

$$I(P_i) = \text{sinc}^2\left(\frac{kl \sin \beta}{2}\right) \text{sinc}^2\left(\frac{kw \sin \alpha}{2}\right) \frac{\sin^2\left[\frac{nk d \sin \alpha}{2}\right]}{\sin^2\left(\frac{kd \sin \alpha}{2}\right)} \cos^2\left(\frac{kw \sin \alpha + \varphi}{2}\right), \quad (2)$$

α 、 β 分别表示沿 x 方向的衍射角和沿 y 方向的衍射角, \vec{k} 表示波矢, w 表示顶反射面和槽反射面的宽度, l 表示光栅的长度, n 表示顶反射面和槽反射面的对数。

$\text{sinc}^2\left(\frac{kl \sin \beta}{2}\right)$ 和 $\text{sinc}^2\left(\frac{kw \sin \alpha}{2}\right)$ 用于描述矩孔衍射因子,零级衍射有最大值; $\frac{\sin^2\left[\frac{nk d \sin \alpha}{2}\right]}{\sin^2\left(\frac{kd \sin \alpha}{2}\right)}$ 用于描述多光束干涉因子,故 MPMG 的光栅方程为

$$d \sin \alpha = m \lambda, d = w + c, m = 0, \pm 1, \pm 2, \dots \quad (3)$$

即光栅的衍射级次分布仅取决于光栅常数 d , d 越大相同级次衍射光的衍射角越大。

$\cos^2\left(\frac{kw \sin \alpha + \varphi}{2}\right)$ 表示凹槽深度引入的附加相位对衍射场强度的调制。

3 MPMG 的衍射特性分析

由式(3)可知,沿 x 轴的衍射场强度分布与光栅常数 d ($d = 2w$)。顶反射面和槽反射面的对数

n 以及凹槽深度 h 有关。图3描述了不同设计参数条件下,夫琅禾费衍射场沿 x 轴的分布图。从图3(a)、3(b)、3(c)可以看出:当仅有槽深是变量时,槽深引入的相位调制使衍射场的能量在0级和 ± 1 级之间转移;当相位差 $\varphi = 2\pi$ 时,夫琅禾费衍射场的能量全部集中在0级,当相位差 $\varphi = \pi$ 时,夫琅禾费衍射场的能量全部集中在 ± 1 级,当 $\varphi = \pi/2, 3\pi/2$ 时,夫琅禾费衍射场的能量平均分布在0级和 ± 1 级。对比图3(a)、3(b)、3(c)可以看出,顶反射面和槽反射面的对数 n 越多,各衍射级次的张角越小,顶反射面和槽反射面的对数 n 与各衍射级次的衍射角大小无关。在讨论光栅常数 $d(d = 2w)$ 对衍射场分布的影响时,为了避免引入波长的影响,选用了 w/λ 。由图3(d)可以看出, w/λ 越大,各衍射级次主极大的角宽度越小,衍射现象越不明显;而且 w/λ 越大,各级衍射级次的衍射角越小。

4 MPMG 的衍射特性测试

在实验室建立了一套评价 MPMG 衍射特性的实验装置。验证装置包括高功率 THz 辐射源系统(图4(a))、THz 激光准直传输系统(图4(b))和光栅测试系统(图4(c))。图4(c)中, Lens 1、Lens 2 构成一组扩束镜,用于表示系统的准直与传输光路; Lens 3、Lens 4、MPMG 与 Lens 5 构成 MPMG 衍射特性的测试光路。实验中使用波长为 1 066~1 078 nm 的可调谐激光器(OPO)和 1 064 nm Nd:YAG 激光器的差频产生高功率 THz 辐射^[13],如图4(a)所示。泵浦激光束的光斑尺寸约为 4 mm。这种由非线性差频效应产生的 THz 激光束与可见、红外激光束不同。对于激光高斯光束,其可以作为平行光进行处理的两个条件是:束腰半径远大于激光波长,波前半径远大于激光波长。前者可确保在激光传输过程中,光斑大小近似不变,后者可确保激光波前近似为平面。THz 激光的波长与束腰尺寸相当,其光斑大小与传输距离近似成正比^[14],通过实验测量,得到自制差频 THz 源的发散角为 12°。因此,实验中使用透镜组来准直 THz 光束,光路图如图4(b)所示,该部分在原理图4(c)中等效为一组扩束镜^[15-16]。

经过透镜组准直后,THz 激光束的发散角为 0.1°。光栅测试系统由 3 个高密度聚乙烯透镜、矩形挡板、MPMG 和 THz 探测器组成,如图4(e)所示。实验中使用的 1D MPMG 由 8 个光栅单元组成,每个光栅单元包括 5 对顶面和槽面。MPMG 的参数如表 1 所示,照片如图4(d)所示。实验中使用的 THz 探测器是从 Advanced Compound Semiconductor Technologies (ACST, Hanau, Germany) 购买的第二代准光学探测器(2dl 12c LS 2500 A1),探测器光敏面封装有直径为 2 mm 的会聚镜,以实现更高的光能收集效率,如图4(f)所示。

试验方法具体为:0.5 THz 辐射经透镜组的准直,平行入射到 MPMG($\theta = 60^\circ, \psi = 0^\circ$)上,并被 MPMG 衍射,衍射波经 THz 透镜汇聚后,在透镜焦平面上用 THz 探测器对 0 级和 ± 1 级衍射波进行检测。在 MPMG 的前表面放置一个很薄的矩形挡板,以确保每次只有一个单元被入射的 THz 波有效地照亮。通过依次移动探测器的位置,记录了 0 级和 ± 1 级的衍射强度。对每个光栅单元重复此操作,得到了所有光栅单元的 0 级和 1 级强度。为了消除激光抖动对测量结果的影响,采用多次测试的方法对测量结果进行了平均,所得结果是 20 次测量的平均值。将所测量数据进行归一化处理,可以得到 8 个光栅单元的 0 阶和 ± 1 阶衍射效率。

通过改变 OPO 的波长,测试了 8 个光栅单元对 0.34 THz 辐射波的衍射光强。光栅单元对 0.5 THz、0.34 THz 辐射的衍射效率理论模拟曲线和测量结果如图 5 所示。由图 5 可见,实验测量结果和理论模拟结果相符合,证明了 MPMG 的衍射特性,即 MPMG 的零级衍射光携带相位信息,其衍射强度由槽深引入的相位调制。

5 结 论

本文介绍了一种 THz 波段的新型 MPMG,它由一系列光栅单元组成,这些光栅单元的槽深梯度与傅立叶变换光谱系统中动镜的不同位置相对应。对 MPMG 的夫琅和费衍射场分布和衍射效率的计算表明,MPMG 的零级衍射光具有相位信息,其衍射强度由槽深引入的相位调制。接着,研制了由 8 个光栅单元组成的 MPMG,对其在

0.5 THz、0.34 THz 下的零级和一级衍射效率进行了测试, 结果与模拟结果吻合较好。由此可知, MPMG 的零级衍射光携带相位信息, 其衍射强度由槽深引入的相位调制。

参考文献:

- [1] ZHANG CH M, LI Q W, YAN Q L, *et al.*. High throughput static channeled interference imaging spectropolarimeter based on a Savart polariscope[J]. *Optics Express*, 2016, 24(20): 23314-23332.
- [2] LUO Y C, LIU X X, HAYTON D J, *et al.*. Fourier phase grating for THz multi-beam local oscillators[C]. *Proceedings of the 26th International Symposium on Space Terahertz Technology, International Symposium on Space Terahertz Technology*, 2015: 77-78.
- [3] MIRZAEI B, SILVA J R G, LUO Y C, *et al.*. Efficiency of multi-beam Fourier phase gratings at 1.4 THz[J]. *Optics Express*, 2017, 25(6): 6581-6588.
- [4] WANG L, GE SH J, HU W, *et al.*. Tunable reflective liquid crystal terahertz waveplates[J]. *Optical Materials Express*, 2017, 7(6): 2023-2029.
- [5] YANG J, XIA T Y, JING SH CH, *et al.*. Electrically tunable reflective terahertz phase shifter based on liquid crystal[J]. *Journal of Infrared, Millimeter, and Terahertz Waves*, 2018, 39(5): 439-446.
- [6] HALL R T, VRABEC D, DOWLING J M. A high-resolution, far infrared double-beam Lamellar grating interferometer[J]. *Applied Optics*, 1966, 5(7): 1147-1158.
- [7] MANZARDO O, MICHAELY R, SCHÄDELIN F, *et al.*. Miniature lamellar grating interferometer based on silicon technology[J]. *Optics Letters*, 2004, 29(13): 1437-1439.
- [8] YU H B, ZHOU G Y, SIONG C F, *et al.*. An electromagnetically driven lamellar grating based Fourier transform microspectrometer[J]. *Journal of Micromechanics and Microengineering*, 2008, 18(5): 055016.
- [9] 高旭, 李舒航, 马庆林, 等. 光栅精密位移测量技术发展综述[J]. *中国光学*, 2019, 12(4): 741-752.
GAO X, LI SH H, MA Q L, *et al.*. Development of grating-based precise displacement measurement technology[J]. *Chinese Optics*, 2019, 12(4): 741-752. (in Chinese)
- [10] 张敏, 吕金光, 梁静秋, 等. 低阶梯多级微反射镜高度误差分析及制作研究[J]. *中国光学*, 2019, 12(4): 791-803.
ZHANG M, LV J G, LIANG J Q, *et al.*. Error analysis and fabrication of low-stepped mirrors[J]. *Chinese Optics*, 2019, 12(4): 791-803. (in Chinese)
- [11] 吴言枫, 王延杰, 孙海江, 等. 复杂动背景下的“低小慢”目标检测技术[J]. *中国光学*, 2019, 12(4): 853-865.
WU Y F, WANG Y J, SUN H J, *et al.*. LSS-target detection in complex sky backgrounds[J]. *Chinese Optics*, 2019, 12(4): 853-865. (in Chinese)
- [12] 中国科学院上海技术物理研究所. 一种太赫兹一维立体相位光栅: 中国, CN106125176B[P]. 2018-06-26.
Shanghai Institute of Technical Physics of the Chinese Academy of Sciences, CAS. Terahertz one-dimensional stereo phase grating: CN, CN106125176B[P]. 2018-06-26. (in Chinese)
- [13] HUANG J G, HUANG ZH M, TONG J CH, *et al.*. Intensive terahertz emission from GaSe_{0.91}S_{0.09} under collinear difference frequency generation[J]. *Applied Physics Letters*, 2013, 103(8): 081104.
- [14] YANG Q J, HE ZH P, SHU R. Lens design and verification used for terahertz space transmission[J]. *Journal of Infrared and Millimeter Waves*, 2017, 36(5): 519-525.
- [15] HUANG Z M, HUANG J G, GAO Y Q, *et al.*. High-resolution terahertz spectrometer with up to 110 m single-pass base[C]. *Proceedings of 2016 IEEE International Conference on Infrared, Millimeter, and Terahertz Waves, IEEE*, 2016: 1-2.
- [16] XIAO ZH Y, YANG Q J, HUANG J G, *et al.*. Terahertz communication windows and their point-to-point transmission verification[J]. *Applied Optics*, 2018, 57(27): 7673-7680.

作者简介:



Yang Qiu-jie (1988—), male, born in Gongyi City, Henan province. Ph.D. He is now an assistant researcher at Shanghai Institute of Technical Physics, and mainly engaged in THz spectral imaging research. E-mail: yqj488112gxx@163.com

杨秋杰(1988—),男,河南巩义人,博士,助理研究员,2017年于中国科学院大学获得博士学位,主要从事THz光谱成像方面的研究。E-mail: yqj488112gxx@163.com



He Zhiping (1977—), male, born in Xinyu City, Jiangxi Province. Ph.D. He is now a researcher and doctoral supervisor of Shanghai Institute of Technical Physics. He is mainly engaged in the research of photoelectric detection and imaging, focusing on the spectral imaging detection technology oriented to lunar and deep space exploration applications and the spaceborne active and passive composite optical technology. E-mail: hzping@mail.sitp.ac.cn

何志平(1977—),男,江西新余人,博士,研究员,博士生导师,2009年于中国科学院获得博士学位,主要研究领域为光电探测与成像,聚焦面向月球及深空探测应用的光谱成像探测技术,以及空间主被动复合光学技术的研究。E-mail: hzping@mail.sitp.ac.cn